Biochimica et Biophysica Acta (BBA) - Molecular Cell Research
Volume 1843, Issue 11, November 2014, Pages 2414–2423

Soluble components of the flagellar export apparatus, FliI, FliJ, and FliH, do not deliver flagellin, the major filament protein, from the cytosol to the export gate

Ráchel Sajó [a], Károly Liliom [a], Adél Muskotál [b], Ágnes Klein [b], Péter Závodszky [a], Ferenc Vonderviszt [b,1], József Dobó [a,1,*]

[a] Institute of Enzymology, Research Centre for Natural Sciences, Hungarian Academy of Sciences, Magyar Tudósok krt. 2, H-1117, Budapest, Hungary

[b] Bio-Nanosystems Laboratory, Faculty of Information Technology, University of Pannonia, Egyetem u. 10, H-8200, Veszprém, Hungary

[1] J. Dobó and F. Vonderviszt co-supervised this research

[*] Corresponding author. Tel.: +36-1-3826768, Fax: +36-1-3826295, E-mail address: dobo.jozsef@ttk.mta.hu

Abbreviations:

FliI, a soluble ATPase component of the flagellar export apparatus; FliH and FliJ, soluble regulatory components of the export apparatus; FliC, flagellin, the major filament protein; FliS, chaperone for FliC; T3SS, type III secretion system; FlhA, FlhB, FliO, FliP, FliQ and FliR, membrane components of the flagellar export apparatus; FlgK and FlgL, hook-filament junction proteins; FlgN, chaperone for FlgK and FlgL; FliD, filament-cap protein; FliT, chaperone for FliD; FliN, a C-ring protein;

Footnote:

Complexes with defined stoichiometry (e. g. FliC:FliS) are indicated with a colon (:), while complexes with varying or unknown stoichiometry (e.g. FliI-FliJ-FliH) are indicated with hyphen (-).

Abstract

Flagella, the locomotion organelles of bacteria, extend from the cytoplasm to the cell exterior. External flagellar proteins are synthesized in the cytoplasm and exported by the flagellar type III secretion system. Soluble components of the flagellar export apparatus, FliI, FliH, and FliJ, have been implicated to carry late export substrates in complex with their cognate chaperones from the cytoplasm to the export gate. The importance of the soluble components in the delivery of the three minor late substrates FlgK, FlgL (hook-filament junction) and FliD (filament-cap) has been convincingly demonstrated, but their role in the transport of the major filament component flagellin (FliC) is still unclear.

We have used continuous ATPase activity measurements and quartz crystal microbalance (QCM) studies to characterize interactions between the soluble export components and flagellin or the FliC:FliS substrate-chaperone complex. As controls, interactions between soluble export component pairs were characterized providing K_d values. FliC or FliC:FliS did not influence the ATPase activity of FliI alone or in complex with FliH and/or FliJ suggesting lack of interaction in solution. Immobilized FliI, FliH, or FliJ did not interact with FliC or FliC:FliS detected by QCM. The lack of interaction in the fluid phase between FliC or FliC:FliS and the soluble export components, in particular with the ATPase FliI, suggests that cells use different mechanisms for the export of late minor substrates, and the major substrate, FliC. It seems that the abundantly produced flagellin does not require the assistance of the soluble export components to efficiently reach the export gate.

Keywords: type III secretion; flagellar export; FliI ATPase; flagellin; late export substrate; FliS chaperone

1. Introduction

Flagella are the locomotion organelles of bacteria. The flagellum consists of three major parts: the basal body (including the rod), the hook, and the filament. Assembly of the flagellum requires the coordinated expression and transport of about 20 structural components, and numerous other proteins play a role in the regulation of the assembly process [1-3]. Outer components of the flagellum starting with the rod proteins are transported to the assembly site by a specialized type III export apparatus [4], which is related to the type III secretion system (T3SS) for virulence factors of certain pathogenic bacteria [5].

The flagellar T3SS of *Salmonella enterica* serotype *typhimurium* (*S. typhimurium*) is composed of six membrane proteins (FlhA, FlhB, FliO, FliP, FliQ, FliR) forming the export gate, which is found within the MS ring of the basal body [4, 6]. Three additional proteins FliI, FliH, and FliJ constitute the soluble components of the export apparatus. Export substrates are thought to be delivered from the cytosol to the export gate by the soluble components [3, 7], which also play a role in recycling of export chaperones [8].

FliI is an ATPase that was shown to be related to the α and β subunits of the F_0F_1 ATP synthase by sequence similarity [9]. The structure of FliI confirmed the homology [10], and based on biochemical and electron microscopic data the functional form of FliI seems to be a homohexamer [11-13] analogous to the $\alpha_3\beta_3$ hexamer ring of the F_1 ATPase. For a long time it was widely believed that FliI provides the energy for the flagellar export system [9, 14, 15]. This assumption was further supported by mutations at the nucleotide-binding site that markedly reduce the ATPase activity of FliI and motility of the cells [14, 16]. Later it turned out that the proton motive force (PMF) is the driving force of the flagellar export apparatus [17, 18] and FliI along with FliH is not absolutely essential for export although their absence results in a highly paralyzed filament formation [19].

FliH also shows sequence similarity to F_0F_1 ATP synthase subunits, namely to the b and δ subunits [20]. Originally FliH was thought to be the regulator of FliI, because it reduces its ATPase activity potentially preventing futile ATPase hydrolysis in the cytosol [15]. However, null mutation of FliH can be substantially bypassed by overexpressing FliI or certain FlhA or FlhB mutations [21], and now it seems likely that FliH is primarily required for anchoring the FliI hexamer to the export gate [1]. Interestingly overexpression of FliH in otherwise wild-type cells also reduces motility [22], which can be explained by the excessive

formation of a FliI:$FliH_2$ heterotrimer [15] preventing FliI hexamerization. In all, FliI and FliH are both required for efficient export, and they also must be expressed in a proper ratio.

Originally FliJ was thought to function as a general chaperone [23]. A recent structural work established that it is homologous to the γ subunit of the F_0F_1 ATP synthase [13] and probably functions as an integral component of the FliI-FliJ-FliH ATPase complex. FliJ is essential for efficient flagellar export, lack of FliJ results in a leaky motile phenotype [23]. Similarly to FliH, overexpression of FliJ in otherwise wild-type cells also reduces motility [22] possibly because it may form 1:1 complexes with FliI when too much FliJ is present [13] preventing the formation of the functional FliI hexamer ring.

The soluble components (FliI, FliH, FliJ) were identified to preferentially associate with membranes [8, 11, 24]. FliI interacts *in vitro* strongly with acidic phospholipids, which in turn promote hexamerization and increase the ATPase activity of FliI [11, 24]. However, on electronmicroscopic images the FliI hexameric ring structure seems to be located under a (likely nonameric) ring formed by the cytoplasmic domains ($FlhA_C$) of FlhA molecules [25, 26] further from the inner membrane. FliI, FliJ, and FliH were all shown to interact with $FlhA_C$ [1] and FliH also binds to the C-ring protein FliN [27] that is thought to play an important role in the localization of the ATPase complex.

FliJ was also shown to have a moonlighting role to cycle export chaperones FlgN (chaperone for hook-filament junction proteins FlgK and FlgL) and FliT (chaperone for filament cap protein FliD), but not FliS, the chaperone of the major filament protein, FliC (flagellin) [8]. FliS binds to the disordered C-terminal part of FliC [28], while the N-terminal disordered segment of FliC carries the export signal of flagellin [29, 30].

FliI (alone or in complex with FliH) was shown to interact with FlgN-FlgK and FlgN-FlgL chaperone-substrate complexes in solution [7], and FliT or the FliT:FliD complex was shown to bind FliI [31]. These observations led to the idea that export substrates are escorted from the cytoplasm to the export gate by the soluble export components. This mechanism seems to be justified for the minor late substrates FlgK, FlgL (hook-filament junction) and FliD (filament-cap), but in the case of the major filament component flagellin (FliC) data are contradictory [15, 22, 32]. An earlier report showed that FliC interacts with FliI and increases its ATPase activity [32], suggesting a role for the FliI-FliC interaction in the export process. Others could not reproduce this ATPase activity enhancement by FliC in the presence or absence of FliH [15] and suggested that other components (e.g. FliJ) might be required. Affinity blots showed that FliC interacts with the soluble export components, FliI, FliH, and FliJ [22], but these interactions were not confirmed by other, more reliable methods. In all, it

is assumed that the soluble export components deliver substrate-chaperone complexes of late substrates from the cytoplasm to the export gate, however this assumption was convincingly demonstrated only for the three minor late substrates FlgK, FlgL (hook-filament junction) and FliD (filament-cap). Fig.1 summarizes the current view of substrate delivery.

In this study our aim was to clarify the role of the soluble components of the flagellar export apparatus in the recognition and delivery of the major export substrate, flagellin. We used a continuous ATPase activity assay to detect changes in FliI activity in the presence or absence of the other two components, FliH and FliJ, upon the addition of FliC or the FliC:FliS complex. To detect physical interaction, regardless of the activity change, quartz crystal microbalance (QCM) measurements were carried out. No interaction was detected between FliC or the FliC:FliS complex and the soluble components in solution by any of the applied methods. We came to the conclusion that, in contrast to minor late export substrates where such mechanism was convincingly demonstrated, the soluble components of the flagellar export system do not deliver flagellin from the cytoplasm to the export gate.

2. Materials and Methods

2.1 Genes and strains

The genes encoding N-terminally His_6-tagged FliJ, FliH and FliS were produced by PCR amplification using genomic DNA from the wild-type *S. typhimurium* strain SJW1103 [33]. The genomic DNA was purified using the NucleoSpin Tissue DNA isolation kit (Macherey-Nagel GmbH). The amplified DNA fragments were cloned into the pET17b vector (Novagen-Merck) between the NdeI and HindIII sites for FliJ and FliH, and the NdeI and XhoI sites for FliS. The gene encoding FliI was also amplified from genomic DNA and cloned into the pET19b vector (Novagen-Merck) between the NdeI and BamHI sites. The final FliI construct encodes a vector derived tag including a His_{10} sequence. All PCR primers are listed in Table 1. Finally the plasmids were transformed into *E. coli* BL21(DE3)pLysS (Novagen-Merck) cells for expression.

2.2 Protein expression and purification

FliC was purified as previously described [34] with some modifications as follows. 3 × 100 mL of *S. typhimurium* SJW1103 culture was grown for 8 hours at 37 °C and 250 rpm in 3% YE (yeast extract solution) medium. 3 × 1 L of 5% YE medium in 3-liter Erlenmeyer

flasks was inoculated with the 100 mL cultures and 0.015% (final concentration) antifoam A (Sigma) was added. The cultures were grown for 16 hours at 37 °C and 80 rpm with aeration using a sparger. 2% PEG-6000 and 1% NaCl (final concentrations) were added to the cultures in order to aggregate detached flagella, then they were shaken for an additional hour at 37°C without aeration. The cells were collected by centrifugation at 6 °C, 30 min, 4400 g, then the pellet was resuspended in 30 mL 20 mM Tris, 150 mM NaCl, pH=7.8. Flagella were detached by shearing the cells using a blender with continuous cooling on ice, then the cells were removed by centrifugation at 6°C, 30 min, 10'000 g. Flagella were collected by centrifuging the supernatant at 10°C, 60 min, 178'000 g (40'000 rpm, T-647.5 rotor, Thermo Scientific). The pellet was washed with 5 mL 20 mM Tris, 150 mM NaCl, pH=7.8, then resuspended in 5 mL 20 mM Tris, pH=7.8 buffer containing a Complete ULTRA mini EDTA-free protease inhibitor cocktail tablet (Roche). Flagella were monomerized by heat treatment at 65°C for 10 min. The aggregates were removed by centrifugation at 4°C, 30 min, 340'000 g (70'000 rpm, MLA-80 rotor, Beckman). Flagellin was purified by polymerization by adding $(NH_4)_2SO_4$ to a final concentration of 0.8 M, then washed twice with 3 mL buffer containing 20 mM Tris, 150 mM NaCl, pH=7.8. The flagellin filaments were resuspended in 3 mL buffer containing 20 mM Tris, 1 mM EDTA, pH=7.8, monomerized again, then purified by anion-exchange chromatography in the same buffer using a linear gradient of 50-150 mM NaCl. Fractions containing FliC were combined, then dialyzed overnight against a buffer containing 20 mM Tris, 50 mM NaCl, 1 mM EDTA, pH=7.8.

FliI, FliJ, FliH, FliS were grown in LB medium until they reached OD_{600}=0.6, and subsequently induced with 0.4 mM (final) IPTG. After induction the cells were grown overnight at 25°C, 180 rpm. The cells were harvested by centrifugation and disrupted by ultrasonic treatment. In the case of FliI, FliJ, and FliH the soluble fraction contained the protein of interest, while FliS formed inclusion bodies.

FliI was purified using a Ni-Sepharose High Performance column (GE Healthcare) in solutions containing 500 mM NaCl using a linear gradient of 30–500 mM imidazole (pH=7.5). Fractions containing FliI were combined, then dialyzed overnight against a buffer containing 20 mM Tris, 200 mM NaCl, 1 mM EDTA, pH=7.8.

FliH was purified using a Ni-NTA Superflow column (Qiagen) in solutions containing 500 mM NaCl using a linear gradient of 10–500 mM imidazole (pH=7.5). Fractions containing FliH were combined and dialyzed overnight against a buffer containing 20 mM Tris, 20 mM NaCl, 1 mM EDTA, pH=7.5. The dialyzed fractions were loaded onto a Source 30Q column (GE Healthcare) and the bound FliH was eluted by a linear gradient of 200-600

mM NaCl in 20 mM Tris, 1 mM EDTA, pH=7.5 buffer, and the fractions containing FliH were combined. The protein eluted at approx. 400 mM NaCl (in 20 mM Tris, 1 mM EDTA, pH=7.5).

FliJ was purified using a Ni-NTA Superflow column as FliH. Fractions containing FliJ were combined and dialyzed against a buffer containing, 50 mM NaCl, 10 mM Na-phosphate, 0.5 mM EDTA, pH=7.0, then loaded onto a Source15S column (GE Healthcare). The bound protein was eluted using a 50-500 mM NaCl gradient, and the fractions containing FliJ were combined. The protein eluted at approx. 250 mM NaCl (in 10 mM Na-phosphate, 0.5 mM EDTA, pH=7.0).

FliS inclusion bodies were washed three times with 50 mM Tris, 1 mM EDTA, 0,5% TritonX-100, pH=8.0, then dissolved overnight at 4 °C in 6 M guanidin-hydrochloride, 10 mM imidazole, pH=7.5. The solubilized protein was loaded onto a Ni-NTA Superflow (Qiagen) column and eluted by a linear gradient of 10–250 mM imidazole, pH=7.5, in 6 M guanidin-hydrochloride, and fractions containing FliS were combined. FliS was refolded by overnight dialyzation at 4 °C in a buffer containing 20 mM Tris, 1 mM EDTA, 200 mM NaCl, (pH=7.5). FliS was further purified on a Superose 12 gel filtration column (GE Healthcare) in a buffer containing 20 mM Tris, 400 mM NaCl, 1 mM EDTA, pH=8.0, and 20% glycerol (to prevent aggregation).

The protein purities were checked by SDS-PAGE (12.5% Laemmli gels), and the oligomeric status was checked by native PAGE using either 7.5% or 10% gels without SDS or 4-15% Mini Protean TGX (BioRad) gradient gels in combination with 25 mM Tris, 192 mM glycine, pH=8.3 as running buffer. All purified proteins were concentrated on 3-kDa-cutoff spin-concentrators, then stored frozen in aliquots.

2.3 ATPase activity measurements

ATPase activity measurements were carried out using a continuous NADH-coupled spectrophotometric assay based on the method of Kiianitsa et al. [35]. FliI (0.4-1 μM) in the presence or absence of other components (FliC, FliJ, FliH, FliS, as indicated in the Results) was preincubated at 30°C for 5 minutes in a buffer containing 25 mM HEPES pH=8.0, 20 mM $MgCl_2$, 0.1 mg/mL BSA, 2 mM DTT, 200 μM NADH (Boehringer Mannheim), 1 mM phosphoenolpyruvate (Sigma), 20 U/mL pyruvate kinase (Sigma), and 40 μg/mL lactate dehydrogenase (Boehringer Mannheim). The reactions were initialized by adding 5 mM

(final) ATP (Sigma). The rate of ATP hydrolysis was monitored by the decrease of NADH absorbance at 340 nm, 30 ^{o}C.

In the presence of phospholipids (PL) the above described protocol was slightly modified. E. coli polar lipid extract (Avanti Polar Lipids) was dissolved in chloroform, dried, then resuspended in 25 mM HEPES pH=8.0 to a 1 mg/mL stock concentration. The suspension was sonicated in a water bath to form liposomes. Phospholipids were added to the reactions in a 10 μg/mL final concentration. BSA and $MgCl_2$ were omitted from the buffer, as BSA and Mg^{2+} caused precipitation of the phospholipids. As Mg^{2+} is necessary for ATPases, the reaction was initialized by adding 5 mM Mg^{2+}-ATP to the reaction. In this case the addition of Mg^{2+}-ATP did not cause any precipitation.

2.4 Quartz Crystal Microbalance (QCM) measurements

QCM directly measures the mass of a compound bound to the sensor, because the mass increase affects the frequency of an oscillating quartz crystal. Using this method a mass difference down to the sub ng range can theoretically be detected [36]. When a protein is immobilized on a quartz crystal sensor chip, and a ligand is injected onto the surface, its association and dissociation are monitored continuously resulting in a frequency change versus time curve, from which the rate constants can be calculated. QCM measurements were performed in an Attana A100 instrument. Biotinylated FliI, FliH and FliJ were prepared by incubating the proteins for 2 h, 25°C with biotinamidohexanoyl-6-aminohexanoic acid N-hydroxysuccinimide ester (Sigma) in 5-fold molar excess, then the unbound biotin was removed by excessive dialyzation against HBS-T buffer (10 mM HEPES, 150 mM NaCl, 0.5 mM EDTA, 0.005% Tween-20, pH=7.5). Biotinylated proteins were immobilized through neutravidin cross-linking on the surface of a biotin coated sensor chip (Attana) according to the manufacturer's instructions in HBS-T buffer. FliI, FliJ, FliH, FliC, FliC:FliS complex and ovalbumin (as negative control) were dialyzed in HBS-T. Equal volumes of the ligands were injected onto the protein coated sensor surfaces. Association and dissociation of the ligands were monitored at a flow rate of 25 μl/min at 20°C. Regeneration of the surface was achieved by injecting 40 μl 2 M KCl, 50 mM NaOH. The kinetic parameters were derived from the obtained data using BIAevaluation software 4.1 (GE Healthcare). Association and dissociation data were fitted simultaneously to a 1:1 Langmuir binding model for FliH on the FliI chip, whereas in all other combinations the two-state reaction (conformational change) model was used where binding was observed. This model describes a 1:1 binding of analyte

to immobilized ligand followed by a conformational change in the complex. Apparent K_d values were calculated as k_{off}/k_{on} for the 1:1 Langmuir binding, and $1/(k_{on}/k_{off}\times(1+ k_{on2}/k_{off2}))$ for the two-state (conformational change) model [37].

3. Results

3.1 Proteins and their interactions detected by native PAGE

Soluble components of the flagellar export apparatus (FliI, FliJ, and FliH) and the flagellin specific chaperone (FliS) were expressed as N-terminally His-tagged proteins in *E. coli* and purified as described in the Materials and Methods. His-tagged versions of the soluble components were previously shown to be fully functional in complementation tests using the appropriate deletion variants of *S. typhimurium* [14, 22], while His-tagged FliS was shown to be functional, as it binds to the C-terminus of its partner FliC [38]. FliC was produced as a native protein and it was used in the monomeric form in our assays. Oligomeric status and interactions between the components were checked by native PAGE. FliI for example was mostly monomeric, but oligomers could be nicely observed on dilute gradient gels (Fig. 2A). The FliI-FliH interaction is detectable by native gel electrophoresis [15], and our native PAGE experiments (data not shown) confirmed this observation, however weaker interactions, like the one between FliI and FliJ, are not detectable by this method (data not shown). We could not detect any interaction between FliI and FliC (Fig. 2A), but because of the above mentioned limitations more sensitive techniques were applied as follows.

3.2 FliC and the FliC:FliS complex do not interact with FliI

In order to clarify the role of the soluble components of the flagellar export apparatus in the recognition of the major export substrate flagellin, first we tested the effect of FliC on the ATPase activity of FliI by a continuous NADH-coupled spectrophotometric assay [35]. Adding up to 30 μM FliC to 1 μM FliI has not shown any significant effect on the ATPase activity of FliI (Fig. 2B). This result is in contrast with a previous study by Silva-Herzog and Dreyfus [32].

FliS acts as the substrate specific chaperone of FliC [39, 40]. We found that FliS is stable in up to 5 μM concentration in the buffer used for the NADH-coupled ATPase activity measurements. In the next experiment we added the FliC:FliS complex (5 μM final) to FliI in

order to determine whether the presence of FliS is required for export substrate recognition. Under these conditions over 90% of FliC and FliS are complexed based on the K_d value determined earlier [41]. We found that the ATPase activity of FliI in the presence or in the absence of FliC:FliS complex showed no significant difference (Fig. 2C). Binding of a protein to FliI does not necessarily influence its ATPase activity as it was demonstrated earlier [31]. Therefore, we carried out QCM and isothermal titration calorimetry (ITC) measurements, which allows us to detect protein-protein binding regardless of the activity change. When tested by ITC we could not detect any interaction between FliI and FliC (data not shown). QCM measurements also confirmed the lack of interaction between FliC or FliC:FliS with FliI (Fig. 3A) as described in the next section.

3.3. QCM results indicate lack of interaction between FliC and individual soluble export components

In order to determine if there is a physical interaction between FliI and FliC, or FliI and the FliC:FliS complex, regardless of the ATPase activity, we immobilized FliI on the surface of a biotin-coated sensor chip through neutravidin cross-linking. FliC or the FliC:FliS complex were injected onto the FliI-coated surface. The association and dissociation pattern did not show any significant binding to FliI, as the signal was comparable to the one obtained for the negative control, ovalbumin (Fig. 3A). These results indicate that FliI by itself does not interact with chaperoned or unchaperoned flagellin. As positive controls FliJ or FliH was injected onto the FliI-coated chip, since both proteins are known to interact with FliI [13, 15]. Both proteins gave large signals indicative of binding to FliI (Fig. 3A) and allowing us to determine the kinetic parameters of association and dissociation, as well as the K_d values (Table 2). A K_d of 274±108 nM was determined for the FliI-FliJ interaction, which is comparable with the EC_{50} value determined with fluid phase activity measurement (see later). The FliI-FliH interaction was measured in two different buffers. In a buffer containing 150 mM NaCl (detailed in the Materials and Methods) the K_d was 309 ± 128 nM, which was surprisingly somewhat higher than the one for FliJ. On the other hand in a buffer composed of 20 mM Tris, 400 mM NaCl, pH=7.5 the interaction was stronger resulting in a K_d of 108 ± 29 nM. Both values were calculated assuming that FliH is dimeric.

We also prepared FliJ-coated and FliH-coated sensor chips. FliI, FliH, FliC, FliC:FliS, or ovalbumin was injected onto the surface with immobilized FliJ. In accordance with the FliI chip results and the ATPase activity measurements, FliI showed binding to FliJ, however the apparent K_d was higher than the other way round. On the other hand FliC, the FliC:FliS

complex and ovalbumin did not bind to FliJ (Fig. 3B). Curiously the FliJ-FliH interaction [42] was not detectable on the FliJ chip possibly because of steric reasons. FliI, FliJ, FliC, FliC:FliS, or ovalbumin was injected onto the FliH-coated sensor chip. FliC, the FliC:FliS complex and ovalbumin did not show significant binding, while FliI (as expected) gave a large signal (Fig. 3C). In this instance the FliJ-FliH interaction was also detectable giving a moderate signal. The calculated K_d values along with the k_{on} and k_{off} rates are listed in Table 2. Overall, the QCM measurements suggest, that FliC or the FliC:FliS complex do not interact with individual soluble components of the export apparatus.

3.4 FliC and FliC:FliS do not interact with FliI in the presence of FliJ and/or FliH

It is known that proper functioning of FliI requires complex formation with FliH and FliJ. Our results show that individual components of the FliI-FliJ-FliH ATPase complex do not interact with chaperoned or unchaperoned FliC. In the following experiments we attempted to gradually reconstitute the ATPase complex and check whether FliC or FliC:FliS has an impact on its activity.

First we added FliJ to FliI and demonstrated that increasing concentrations of FliJ increased the activity of FliI until it reached a plateau of approximately 0.275 min^{-1} (equivalent to 1.67 nmol ADP min^{-1} per µg FliI) (Fig. 4A-B). Similar results were obtained by others [8, 13]. From the FliI-FliJ activity slopes an EC_{50} of 253 ± 33 nM was determined, which is in good agreement with the K_d value obtained on the FliI chip by QCM (Table 2). From these measurements it is not possible to determine the binding stoichiometry, but it is plausible to assume that at high FliJ to FliI ratio 1:1 complexes are dominant, while at low FliJ to FliI ratio FliJ promotes FliI hexamerization, as discussed by Ibuki et al. [13].

To investigate if there is an effect of FliC or FliC:FliS on the FliI-FliJ complex, we measured the activity of the FliI-FliJ complex in the presence of FliC or FliC:FliS. It is plausible to assume that in the functional form one FliJ molecule is surrounded by a FliI hexamer [13], therefore we mixed 1 µM FliI, and 0.16 µM FliJ. We found that 5 µM FliC or 5 µM FliC:FliS did not influence the ATPase activity of FliI-FliJ complex (Fig. 4C). We used 5 µM FliC:FliS because FliS or its complex precipitates at >5 µM during the ATPase measurements. As flagellin monomers are in high abundance within the cell we also tested FliC alone at higher concentrations. Up to 30 µM FliC did not have any significant effect on the activity of the FliI-FliJ complex (data not shown).

Next we checked the effect of FliH on the activity of FliI. Adding FliH to FliI decreased its ATPase activity in accordance with published data [15], but the extent of inhibition was somewhat lower possibly due to the different His-tag applied. Adding a large excess of FliC to FliI-FliH did not cause a significant change in the ATPase activity (Fig. 5A), while adding increasing amounts of FliJ resulted in a sigmoidal curve with an EC_{50} value of 723 ± 85 nM (Fig. 5B).

Next we tested whether the full FliI-FliJ-FliH complex is capable of recognizing flagellin alone or in complex with its chaperone. Two different setups were tested. In one FliI, FliJ, and FliH were mixed in a 6:1:2 molar ratio reflecting the presumed stoichiometry of the ATPase complex. In the other FliI and FliH were mixed in a 1:2 molar ratio, as a FliH dimer can bind to a FliI monomer [15], and FliJ was added in 1/6 molar ratio compared to FliI. Both setups gave essentially the same result. When FliC (5 μM) or FliC:FliS (5 μM) was added to the FliI-FliH-FliJ complex, the ATPase activity was practically the same in the presence or absence of FliC or the FliC:FliS complex. Fig. 5C depicts the results of the first setup. FliC did not cause any significant effect on the ATPase activity of the FliI:FliJ:FliH complex even at 30 μM concentration (data not shown).

3.5 Interactions in the presence of acidic phospholipid liposomes

It is known that FliI, FliJ and FliH have intrinsic membrane affinity [8, 24], and the presence of acidic phospholipids enhances the ATPase activity of FliI as well as its hexamerization [24], hence we investigated whether the presence of phospholipids affects flagellin recognition by the soluble components. We added FliC, FliS or FliC:FliS to FliI in the presence of polar phospholipid liposomes. Neither of the proteins caused any significant change in the ATPase activity of FliI (Fig. 6A). Next, we repeated this experiment but instead of FliI we used the FliI-FliJ complex. Adding FliC to the FliI-FliJ complex in the presence of liposomes did not affect the ATPase activity (Fig. 6B). Surprisingly, adding FliS to FliI-FliJ decreased its ATPase activity approximately to half of the original, and adding the FliC:FliS complex instead of FliS had about the same effect as FliS alone (Fig. 6B). FliH (data not shown) had no influence on the observed effect caused by FliS.

The results indicate that the observed effect depends on FliS, but not on FliC, and only FliS is responsible for the activity decrease of the membrane-bound FliI-FliJ ATPase complex. While there are many questions remaining, it seems plausible to assume that FliS promotes disassembly of the membrane-bound ATPase complex to facilitate flagellin export. A more precise clarification of the role of FliS requires further investigations.

4. Discussion

Previous reports established that chaperoned minor late substrates (FlgK, FlgL, FliD) are recognized by FliI or the FliI-FliH complex [7, 31], and this interaction also takes place in the fluid phase. Hence the general view has been that export substrates are delivered from the cytosol to the export gate by FliI aided by FliH [1-3]. Flagellin (FliC) and also hook protein (FlgE) were shown to stimulate the ATPase activity of FliI [32], but others could not reproduce this effect [15], and suggested that other components, like FliJ, might be required. On the other hand interactions between FliC and FliI, FliH, or FliJ were detected by affinity blots [22], and it was implied, although not unambiguously proven, that FliC is not an exception from the rule, and it is also delivered to the export gate by the soluble components.

In order to clarify the role of the soluble export components in the recognition and delivery of the major filament component, flagellin, we undertook to thoroughly examine the possible interactions between FliC and the soluble export components by activity-based (indirect) and physical (direct) methods.

We have tested the putative enhancement of the ATPase activity of FliI by FliC in nearly every possible combinations. We found that FliC alone or its complex with FliS did not influence the activity of FliI alone, FliI in complex with FliJ, FliI in complex with FliH, or FliI in complex with both FliJ and FliH. It is important to note that the ATPase activity of FliI was sensitive to detect all well-established interactions with the soluble components of the export apparatus. Thus, our activity measurements strongly suggest the lack of interaction between chaperoned or unchaperoned flagellin in the fluid phase with FliI-containing complexes.

We carried out quartz crystal microbalance measurements in order to check if there is a physical interaction regardless of the ATPase activity between FliC and any of FliI, or FliJ, or FliH. Again, we could not detect significant binding of FliC or FliC:FliS to immobilized individual components. QCM measurements confirmed that there is no interaction between FliC or FliC:FliS and the soluble components in the fluid phase. These measurements enabled us to determine the strength of the interactions between pairs of the soluble components of the export apparatus (Table 2). Particularly interesting is the FliI-FliJ interaction where the determined EC_{50} value based on the activity assay, and the K_d value obtained by QCM on the FliI chip are nearly identical.

Our results imply that the soluble components of the export apparatus, FliI, FliJ, FliH, and their complexes do not bind FliC or FliC:FliS in the cytosol, hence they do not deliver flagellin to the membrane-embedded export machinery, however, we cannot exclude the possibility that they facilitate translocation of flagellin at the export gate. It is noteworthy that FliS or FliC:FliS decreased the ATPase activity of FliI-FliJ but only in the presence of liposomes. Based on this observation it seems plausible that FliS promotes the disassembly of the membrane-bound ATPase complex, however it requires further experiments to clarify the role of FliS in this scenario. Interestingly FliS might have a role in the transcriptional regulation of flagellin as well, since FliS interacts with the anti-sigma factor FlgM, which inhibits FliA, a flagellar-specific sigma factor [43].

Based on our results it is presumable that flagellin is exported by a different mechanism than the other three late substrates. Minor late substrates (FlgK, FlgL, FliD) are built into the filament in well-defined, low copy numbers. Hook-filament junction proteins (FlgK, FlgL) are found in 11 copies each, and the filament capping protein (FliD) forms a pentameric complex at the tip [2, 44]. All these three components are required for the assembly of the flagellum, and their export must precede the export of the high abundance flagellin, which has a copy number of about 20’000 [44]. It seems plausible that chaperoned minor late substrates require a facilitated delivery by the soluble export components in order to compensate for their low concentration and ensure that they are exported before FliC [45]. Evans et al. [8] had a similar conclusion based on their observation that FliJ escorts chaperones for the minor filament components, but not for flagellin. Recently, from a different aspect, Bange et al. [46] proposed a mechanism by which the flagellar T3SS switches from the stoichiometric export of FliD to the high-throughput export of flagellin, emphasizing the role of FliJ in the stoichiometric export. Images of Salmonella deficient for all FliI, FliH, and FliJ (*ΔfliHIJ*) showed rare flagellation (<1%) [18], but the length of the occasionally formed flagella seemed to be normal. This observation can be explained that without aided delivery, minor late components are exported only rarely by chance, but once these structural components are in place, mass export of flagellin occurs almost normally, probably by simple diffusion, without the need for the soluble export components.

In all, the lack of interaction in the fluid phase between FliC or FliC:FliS with the soluble export components indicates that these components do not deliver flagellin to the export gate, and our observations combined with recent studies suggest that the mechanism for the mass export of flagellin is different from the aided delivery of minor late substrates.

Acknowledgements

This work was supported by the Hungarian Scientific Research Fund (OTKA) grants K104726 and NK108642, and the János Bolyai Research Fellowship of the Hungarian Academy of Sciences.

References

1. T. Minamino, Protein export through the bacterial flagellar type III export pathway, *Biochim. Biophys. Acta.* **1843** (2014) 1642-1648
2. F.F. Chevance, K.T. Hughes, Coordinating assembly of a bacterial macromolecular machine, *Nat. Rev. Microbiol.* **6** (2008) 455-465.
3. T. Minamino, K. Imada, K. Namba, Molecular motors of the bacterial flagella, *Curr. Opin. Struct. Biol.* **18** (2008) 693-701.
4. R.M. Macnab, Type III flagellar protein export and flagellar assembly, *Biochim. Biophys. Acta.* **1694** (2004) 207-217.
5. J.E. Galán, H. Wolf-Watz, Protein delivery into eukaryotic cells by type III secretion machines, *Nature* **444** (2006) 567-573.
6. Minamino T, Macnab RM. Components of the Salmonella flagellar export apparatus and classification of export substrates. *J. Bacteriol.* **181** (1999) 1388-1394.
7. J. Thomas, G.P. Stafford, C. Hughes, Docking of cytosolic chaperone-substrate complexes at the membrane ATPase during flagellar type III protein export, *Proc. Natl. Acad. Sci. U.S.A.* **101** (2004) 3945-3950.
8. L.D. Evans, G.P. Stafford, S. Ahmed, G.M. Fraser, C. Hughes, An escort mechanism for cycling of export chaperones during flagellum assembly, *Proc. Natl. Acad. Sci. U.S.A.* **103** (2006) 17474-17479.
9. A.P. Vogler, M. Homma, V.M. Irikura, R.M. Macnab, Salmonella typhimurium mutants defective in flagellar filament regrowth and sequence similarity of FliI to F_0F_1, vacuolar, and archaebacterial ATPase subunits, *J. Bacteriol.* **173** (1991) 3564-3572.
10. K. Imada, T. Minamino, A. Tahara, K. Namba, Structural similarity between the flagellar type III ATPase FliI and F_1-ATPase subunits, *Proc. Natl. Acad. Sci. U.S.A.* **104** (2007) 485-490.
11. L. Claret, S.R. Calder, M. Higgins, C. Hughes, Oligomerization and activation of the FliI ATPase central to bacterial flagellum assembly, *Mol. Microbiol.* **48** (2003) 1349-1355.
12. K. Kazetani, T. Minamino, T. Miyata, T. Kato, K. Namba, ATP-induced FliI hexamerization facilitates bacterial flagellar protein export, *Biochem. Biophys. Res. Commun.* **388** (2009) 323-327.
13. T. Ibuki, K. Imada, T. Minamino, T. Kato, T. Miyata, K. Namba, Common architecture of the flagellar type III protein export apparatus and F- and V-type ATPases, *Nature Struct. Mol. Biol.* **18** (2011) 277-282.
14. F. Fan, R.M. Macnab, Enzymatic characterization of FliI. An ATPase involved in flagellar assembly in Salmonella typhimurium, *J. Biol. Chem.* **271** (1996) 31981-31988.
15. T. Minamino, R.M. Macnab, FliH, a soluble component of the type III flagellar export apparatus of Salmonella, forms a complex with FliI and inhibits its ATPase activity, *Mol. Microbiol.* **37** (2000) 1494-1503.
16. G. Dreyfus, A.W. Williams, I. Kawagishi, R.M. Macnab, Genetic and biochemical analysis of Salmonella typhimurium FliI, a flagellar protein related to the catalytic

subunit of the F_0F_1 ATPase and to virulence proteins of mammalian and plant pathogens, *J. Bacteriol.* **175** (1993) 3131-3138.

17. T. Minamino, K. Namba, Distinct roles of the FliI ATPase and proton motive force in bacterial flagellar protein export, *Nature* **451** (2008) 485-488.
18. K. Paul, M. Erhardt, T. Hirano, D.F. Blair, K.T. Hughes, Energy source of flagellar type III secretion, *Nature* **451** (2008) 489-492.
19. T. Minamino, Y.V. Morimoto, N. Hara, K. Namba, An energy transduction mechanism used in bacterial flagellar type III protein export. *Nat. Commun.* **2** (2011) 475.
20. M.J. Pallen, C.M. Bailey, S.A. Beatson, Evolutionary links between FliH/YscL-like proteins from bacterial type III secretion systems and second-stalk components of the F_oF_1 and vacuolar ATPases, *Protein Sci.* **15** (2006) 935-941.
21. T. Minamino, B. González-Pedrajo, M. Kihara, K. Namba, R.M. Macnab, The ATPase FliI can interact with the type III flagellar protein export apparatus in the absence of its regulator, FliH, *J. Bacteriol.* **185** (2003) 3983-3988.
22. T. Minamino, R.M. Macnab, Interactions among components of the Salmonella flagellar export apparatus and its substrates, *Mol. Microbiol.* **35** (2000) 1052-1064.
23. T. Minamino, R. Chu, S. Yamaguchi, R.M. Macnab, Role of FliJ in flagellar protein export in Salmonella, *J. Bacteriol.* **182** (2000) 4207-4215.
24. F. Auvray, A.J. Ozin, L. Claret, C. Hughes, Intrinsic membrane targeting of the flagellar export ATPase FliI: interaction with acidic phospholipids and FliH, *J. Mol. Biol.* **318** (2002) 941-50.
25. S. Chen, M. Beeby, G.E. Murphy, J.R. Leadbetter, D.R. Hendrixson, A. Briegel, Z. Li, J. Shi, E.I. Tocheva, A. Müller, M.J. Dobro, G.J. Jensen, Structural diversity of bacterial flagellar motors, *EMBO J.* **30** (2011) 2972-2981.
26. P. Abrusci, M. Vergara-Irigaray, S. Johnson, M.D. Beeby, DR Hendrixson, P Roversi, Friede ME, Deane JE, Jensen GJ, Tang CM, Lea SM, Architecture of the major component of the type III secretion system export apparatus. *Nat. Struct. Mol. Biol.* **20** (2013) 99-104
27. T. Minamino, S.D. Yoshimura, Y.V. Morimoto, B. González-Pedrajo, N. Kami-Ike, K. Namba, Roles of the extreme N-terminal region of FliH for efficient localization of the FliH-FliI complex to the bacterial flagellar type III export apparatus, *Mol. Microbiol.* **74** (2009) 1471-1483.
28. A.G. Evdokimov, J. Phan, J.E. Tropea, K.M. Routzahn, H.K. Peters, M. Pokross, D.S. Waugh, Similar modes of polypeptide recognition by export chaperones in flagellar biosynthesis and type III secretion, *Nat. Struct. Biol.* **10** (2003) 789-793.
29. B.M. Végh, P. Gál, J. Dobó, P. Závodszky, F. Vonderviszt, Localization of the flagellum-specific secretion signal in Salmonella flagellin, Biochem Biophys Res Commun. **345** (2006) 93-98.
30. J. Dobó, J. Varga, R. Sajó, B.M. Végh, P. Gál, P. Závodszky, F. Vonderviszt, Application of a short, disordered N-terminal flagellin segment, a fully functional flagellar type III export signal, to expression of secreted proteins, *Appl. Environ. Microbiol.* **76** (2010) 891-899.

31. T. Minamino, M. Kinoshita, K. Imada, K. Namba, Interaction between FliI ATPase and a flagellar chaperone FliT during bacterial flagellar protein export, *Mol. Microbiol.* **83** (2012) 168-178.

32. E. Silva-Herzog, G. Dreyfus, Interaction of FliI, a component of the flagellar export apparatus, with flagellin and hook protein, *Biochim. Biophys. Acta* **1431** (1999) 374-383.

33. S. Yamaguchi, H. Fujita, K. Sugata, T. Taira, T. Iino, Genetic analysis of H2, the structural gene for phase-2 flagellin in Salmonella, *J. Gen. Microbiol.* **130** (1984) 255-265.

34. F. Vonderviszt, S. Kanto, S.-I. Aizawa, K. Namba, Terminal regions of flagellin are disordered in solution, *J. Mol. Biol.* **209** (1989) 127–133.

35. K. Kiianitsa, J.A. Solinger, W.D. Heyer, NADH-coupled microplate photometric assay for kinetic studies of ATP-hydrolyzing enzymes with low and high specific activities, *Anal. Biochem.* **321** (2003) 266-271.

36. K.A. Marx, Quartz Crystal Microbalance: A useful tool for studying thin polymer films and complex biomolecular systems at the solution-surface interface, *Biomacromolecules* **4** (2003) 1099-1120.

37. C.A. Lipschultz, Y. Li, S. Smith-Gill, Experimental design for analysis of complex kinetics using surface plasmon resonance. *Methods.* **20** (2000) 310-318.

38. A.J. Ozin, L. Claret, F. Auvray, C. Hughes, The FliS chaperone selectively binds the disordered flagellin C-terminal D0 domain central to polymerization, *FEMS Microbiol. Lett.* **219** (2003) 219-224.

39. T. Yokoseki, K. Kutsukake, K. Ohnishi, T. Iino, Functional analysis of the flagellar genes in the fliD operon of Salmonella typhimurium, *Microbiology* **141** (1995) 1715–1722.

40. F. Auvray, J. Thomas, G. Fraser, C. Hughes, Flagellin polymerization control by a cytosolic export chaperone, *J. Mol. Biol*. **308** (2001) 221–229.

41. A. Muskotál, R. Király, A. Sebestyén, Z. Gugolya, B.M. Végh, F. Vonderviszt, Interaction of FliS flagellar chaperone with flagellin. *FEBS Lett.* **580** (2006) 3916-3920.

42. B. González-Pedrajo, G.M. Fraser, T. Minamino, R.M. Macnab, Molecular dissection of Salmonella FliH, a regulator of the ATPase FliI and the type III flagellar protein export pathway, *Mol. Microbiol*. **45** (2002) 967-982.

43. A. Galeva, N. Moroz, Y.H. Yoon, K.T. Hughes, F.A. Samatey, A.S. Kostyukova, Bacterial flagellin-specific chaperone FliS interacts with anti-sigma factor FlgM, *J. Bacteriol.* **196** (2014) 12125-12121.

44. R.M. Macnab, How bacteria assemble flagella, *Annu. Rev. Microbiol.* **57** (2003) 77-100.

45. M. Kinoshita, N. Hara, K. Imada, K. Namba, T. Minamino, Interactions of bacterial flagellar chaperone-substrate complexes with FlhA contribute to co-ordinating assembly of the flagellar filament. *Mol. Microbiol.* **90** (2013) 1249-1261.

46. G. Bange, N. Kümmerer, C. Engel, G. Bozkurt, K. Wild, I. Sinning, FlhA provides the adaptor for coordinated delivery of late flagella building blocks to the type III secretion system, *Proc. Natl. Acad. Sci. U. S. A.* **107** (2010) 11295-11300.

Tables

Table 1

Primers used for cloning of *S. typhimurium* genes

Gene	Direction	Sequence
FliJ	forward	5′_gcgcgcCATATG**catcaccaccaccatcac**gcacaacatggcgctctgg_3′
	reverse	5′_gcgcggcAAGCTTtcattcgggtttcctcattgctgc_3′
FliH	forward	5′_gcgcgcgcCATATG**catcaccaccaccatcac**tctaatgaattgccgtgcaag_3′
	reverse	5′_ggaaggAAGCTTtcagagcactcccggcgccg_3′
FliS	forward	5′_gcgcgcCATATG**catcaccaccaccatcac**tacaccgcgagcggtatc_3′
	reverse	5′_cccggaCTCGAGttaacgagactcctggaaagatgc_3′
FliI	forward	5′_acatCATATGaccacgcgcctgac_3′
	reverse	5′_acatCTCGAGtcacaccgtcggga_3′

The restriction sites used for cloning, NdeI (CATATG), HindIII (AAGCTT), and XhoI (CATATG) are in capital letters, the start and stop codons are underlined, while the His_6-tag coding region is bold. For the FliI construct the start codon and His_{10}-tag are encoded by the vector.

Table 2

Summary of the determined k_{on}, k_{off}, and K_d values

Immobilized protein	Injected protein	k_{on} ($M^{-1}s^{-1}$)	k_{off} (s^{-1})	k_{on2} (s^{-1})	k_{off2} (s^{-1})	[c] K_d (nM)
FliI	FliJ	$8.33\pm1.86\times10^{3}$	$3.14\pm0.93\times10^{-2}$	$1.21\pm0.10\times10^{-2}$	$9.51\pm1.00\times10^{-4}$	274±108
	[a] FliH	$2.23\pm0.85\times10^{3}$	$6.89\pm1.15\times10^{-4}$	-	-	309±128
	[b] FliH	$4.46\pm1.02\times10^{3}$	$4.81\pm0.65\times10^{-4}$	-	-	108±29
	FliC	no binding				
	FliC:FliS	no binding				
	ovalbumin	no binding				
FliJ	FliI	$5.21\pm1.5\times10^{3}$	$2.08\pm0.48\times10^{-2}$	$4.57\pm0.38\times10^{-3}$	$1.78\pm0.34\times10^{-3}$	1117±470
	FliH	no binding				
	FliC	no binding				
	FliC:FliS	no binding				
	ovalbumin	no binding				
FliH	FliI	$6.87\pm0.93\times10^{3}$	$9.82\pm0.72\times10^{-3}$	$5.44\pm0.42\times10^{-3}$	$2.61\pm0.55\times10^{-3}$	463±126
	FliJ	$2.20\pm0.70\times10^{4}$	$5.86\pm1.84\times10^{-2}$	$1.29\pm0.48\times10^{-2}$	$2.44\pm1.55\times10^{-3}$	422±363
	FliC	no binding				
	FliC:FliS	no binding				
	ovalbumin	no binding				

Standard deviations of 3 parallel measurements are indicated

[a] Measured in a buffer containing 150 mM NaCl

[b] Measured in a buffer containing 400 mM NaCl

[c] Apparent K_d values were calculated as k_{off}/k_{on} for the 1:1 Langmuir binding, and $1/(k_{on}/k_{off}\times(1+ k_{on2}/k_{off2}))$ for the two-state (conformational change) model

Figure Legends

Fig. 1. Putative mechanism of substrate delivery and a hypothetical model for the flagellar type III export apparatus. The export apparatus is found within the C-ring of the basal body. The FliI:$FliH_2$ complex is thought to deliver chaperoned late substrates from the cytoplasm to the export gate, which is composed of membrane embedded proteins, FlhA, FlhB, FliO, FliP, FliQ, and FliR. FlhA probably forms a nonameric ring [26], part of which is depicted here. FliH docks the FliI hexamer below this ring, but the FliH docking site (shown in red and striped red) is uncertain [1, 26]. Involvement of the soluble components (FliI, FliH, and FliJ) of the flagellar export apparatus has been demonstrated for the delivery of minor late substrates. Whether or not the major substrate, flagellin, is also escorted to the export gate by the same mechanism remains to be seen.

Fig. 2. Lack of interaction of FliI with FliC or FliC:FliS complex. (A) Native (non-denaturing) PAGE of oligomeric FliI and FliI-FliC mixtures. Left: 8 μg of FliI was run on a 4-15% Mini Protean TGX precast gel. Right: the intensity of the FliC band does not change upon the addition of various amounts of FliI. Samples were run on a 10% gel. (B) ATPase activity of FliI alone or in the presence of FliC. Adding FliC to FliI does not significantly affect its ATPase activity. (C) The ATPase activity of FliI alone or in the presence of the FliC:FliS complex. The FliC:FliS complex does not influence the ATPase activity of FliI. All activity measurements were carried out using a continuous NADH-coupled spectrophotometric assay as described in Materials and Methods. Protein concentrations are indicated on the panels. The panels depict representative curves of at least 3 parallel measurements, which applies to all subsequent figures. The rate of ATP hydrolysis was monitored by the decrease of NADH absorbance at 340 nm.

Fig. 3. Binding of flagellar components to immobilized FliI, FliJ, or FliH detected by QCM. Biotinylated FliI, FliJ and FliH were prepared as described in Materials and Methods. They were immobilized on the surface of biotinylated chips through neutravidin cross-linking. Equal volumes (40 μL) of the analytes were injected onto the protein-coated sensor surfaces. Representative measurements showing the association-dissociation curves are presented. (A) 9.9 μM FliJ, 7.1 μM $FliH_2$ (assumed to be dimeric), 13 μM FliC, 6 μM FliC:FliS, or 13 μM ovalbumin (as negative control) was injected onto the surface covered with immobilized FliI.

Binding was observed for FliH and FliJ, while FliC, FliC:FliS and ovalbumin did not bind to FliI. (B) 10 μM FliI, 3.55 μM $FliH_2$, 13 μM FliC, 5.8 μM FliC:FliS, or 13 μM ovalbumin was injected onto the surface covered with immobilized FliJ. FliI bound to immobilized FliJ, while FliC, FliC:FliS and ovalbumin did not. The FliJ-FliH interaction was not detectable on this chip.
(C) 8 μM FliI, 4.6 μM FliJ, 13 μM FliC, 5.8 μM FliC:FliS, or 13 μM ovalbumin were injected onto the surface covered with immobilized FliH. FliI bound to immobilized FliH, while FliC, FliC:FliS and ovalbumin did not. The FliJ-FliH interaction was detectable on this surface.

Fig. 4. The effect of FliJ on the activity of FliI, and the activity of FliI-FliJ in the presence or absence of FliC or FliC:FliS. (A) Adding FliJ to FliI enhances the ATPase activity of FliI in a concentration dependent manner. The initial slope is lower than that in the later phase, possibly because ATP-induced hexamerization (known to promote activity) in the presence of FliJ is probably not instantaneous. Protein concentrations are indicated on the panel. (B) The maximal slopes (multiplied by -1) from panel A were plotted as the function of FliJ concentration, and an EC_{50} of 253 ± 33 nM was determined for the activity enhancement. The error represents the standard error of the fitting. (C) The ATPase activity of FliI plus FliJ in the presence or absence of FliC or FliC:FliS shows no significant difference. Protein concentrations are indicated on the panel. Activity measurements were carried out as described briefly in Fig. 1, and in more detail in the Materials and Methods.

Fig. 5. The activity of various FliI complexes with FliH and FliJ, and their activity in the presence or absence of FliC or FliC:FliS. (A) Adding FliH in a two-fold molar excess to FliI reduced its activity to approximately half. The molar ratios reflect the stoichiometry of the FliI:$FliH_2$ complex [15]. FliC does not significantly affect the ATPase activity of FliI plus FliH. Protein concentrations are indicated on the panel. (B) FliJ at various concentrations (0, 0.16, 0.33, 0.66, 1, 2, 3 μM) was added to a mixture of 1 μM FliI and 2 μM FliH. The ATPase activity increased until it reached a plateau at approximately 3 μM FliJ. Slopes (multiplied by -1) were plotted as the function of FliJ concentration, and an EC_{50} of 723 ± 85 nM was determined for the activity enhancement. The error represents the standard error of the fitting. (C) FliI, FliJ and FliH were mixed at a 6:1:2 molar ratio reflecting the putative stoichiometry of the functional complex, and the ATPase activity was measured. Adding FliC or the

FliC:FliS complex to the FliI-FliJ-FliH mixture has no effect on the ATPase activity. Protein concentrations are indicated on the panel. When FliI, FliJ and FliH were tested at other ratios (data not shown), essentially the same results were obtained, i.e. FliC or FliC:FliS did not influence the activity. Activity measurements were carried out as described in Fig. 1 and the Materials and Methods.

Fig. 6. The activity of FliI and FliI-FliJ in the presence of phospholipids, and their activity in the presence or absence of FliC or FliC:FliS. (A) Adding E. coli polar phospholipid liposomes to FliI increases its ATPase activity (see Fig. 1B for comparison). The ATPase activity of FliI in the presence of phospholipids (10 μg/mL) was not significantly altered by the addition of FliS, FliC or the FliC:FliS complex. (B) The ATPase activity of FliI-FliJ in the presence of phospholipids (10 μg/mL) was not significantly altered by the addition of FliC. The FliC:FliS complex reduced the activity significantly to about half of the original. FliS alone at the same concentration reduced the activity to the same extent as FliC:FliS. FliI and FliJ concentrations were lowered compared to previous measurements, in order to prolong the time until the substrates are consumed, but the FliI-FliJ ratio was kept 6:1 as before. Activity measurements were carried out as described in the Materials and Methods. The reaction was initialized by adding 5 mM Mg-ATP. Protein concentrations are indicated on the panels.

Fig. 1

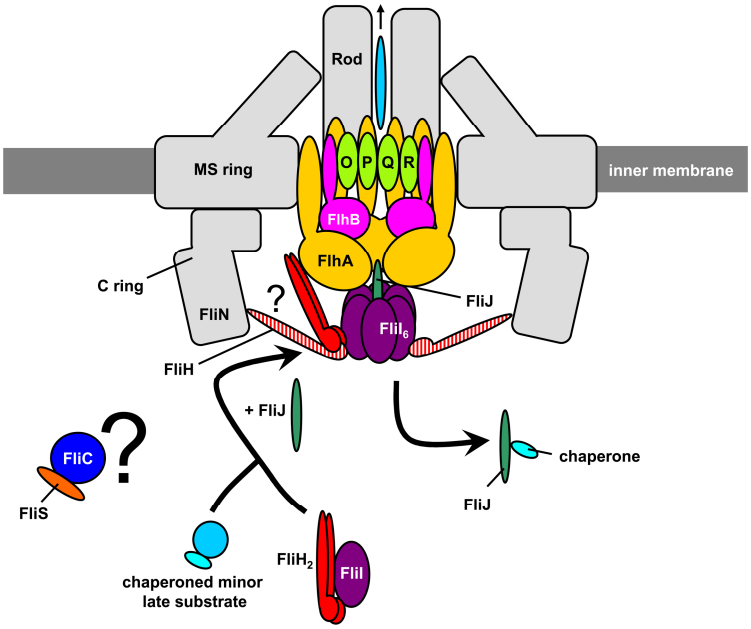
Rod
MS ring
O
P
Q
R
inner membrane
FlhB
FlhA
C ring
FliN
?
FliJ
FliI6
FliH
+ FliJ
FliC
?
FliS
chaperone
FliJ
FliH2
FliI
chaperoned minor
late substrate

Fig. 2

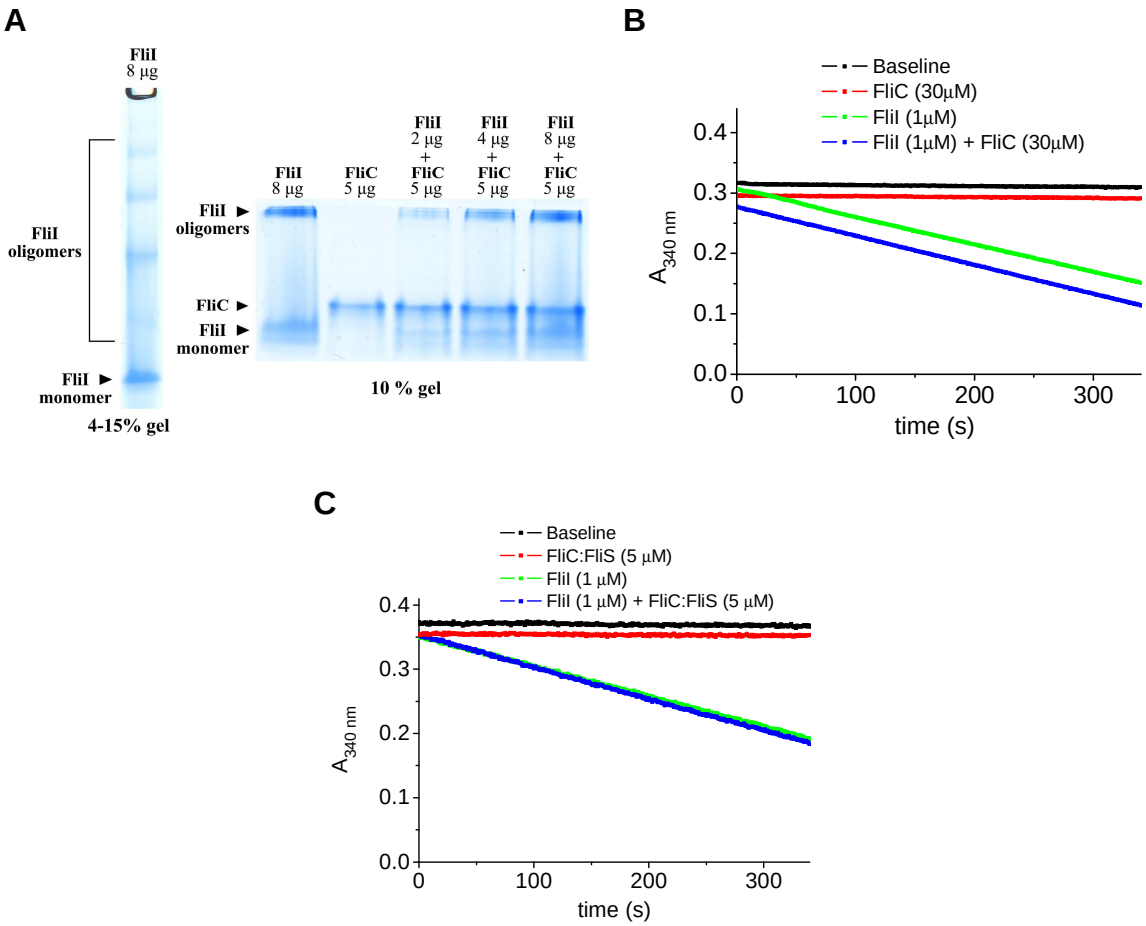
A
FliI
8 µg
FliI
oligomers
FliI ►
monomer
4-15% gel
FliI
8 µg
FliC
5 µg
FliI
2 µg
+
FliC
5 µg
FliI
4 µg
+
FliC
5 µg
FliI
8 µg
+
FliC
5 µg
FliI ►
oligomers
FliC ►
FliI ►
monomer
10 % gel
B
Baseline
FliC (30µM)
FliI (1µM)
FliI (1µM) + FliC (30µM)
A340 nm
0.0
0.1
0.2
0.3
0.4
0
100
200
300
time (s)
C
Baseline
FliC:FliS (5 µM)
FliI (1 µM)
FliI (1 µM) + FliC:FliS (5 µM)
A340 nm
0.0
0.1
0.2
0.3
0.4
0
100
200
300
time (s)

Fig. 3

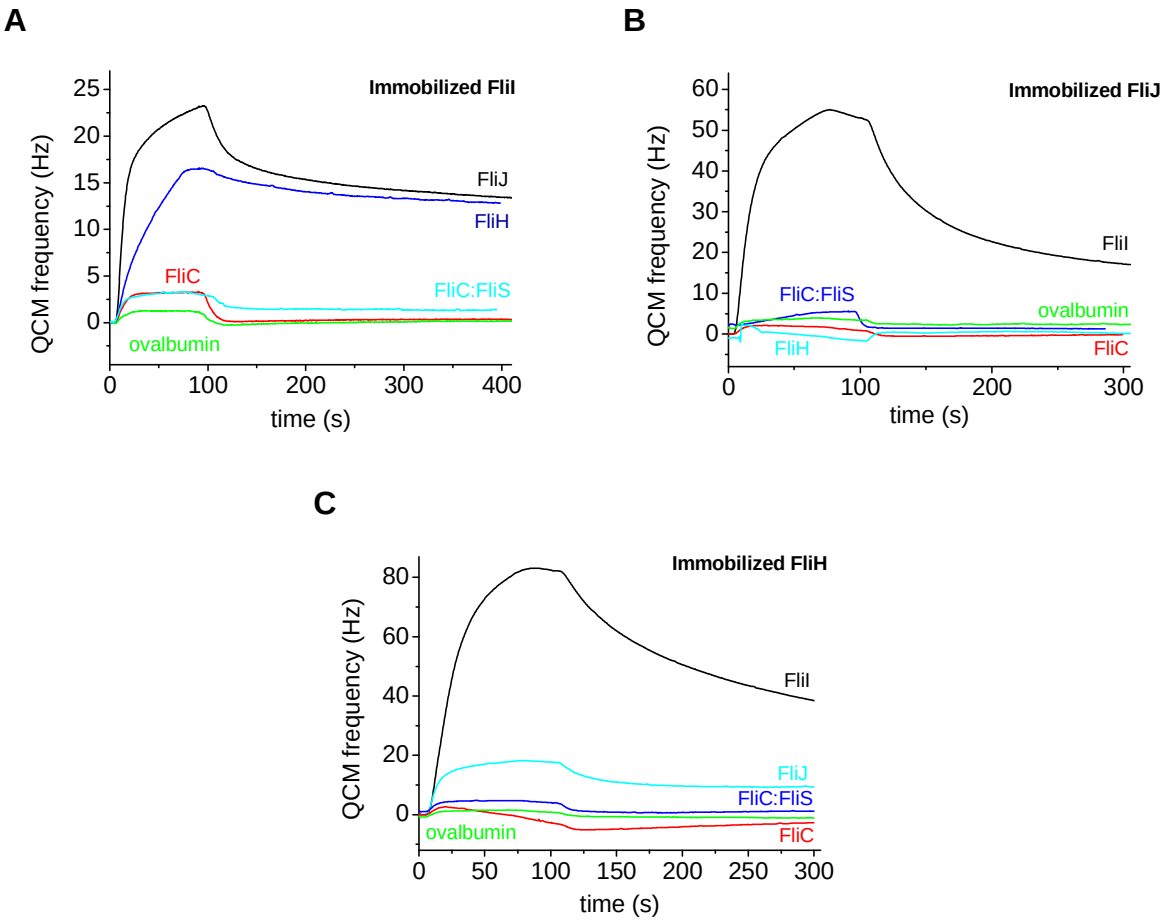
A
Immobilized FliI
QCM frequency (Hz)
time (s)
FliJ
FliH
FliC
FliC:FliS
ovalbumin
B
Immobilized FliJ
QCM frequency (Hz)
time (s)
FliI
FliC:FliS
ovalbumin
FliH
FliC
C
Immobilized FliH
QCM frequency (Hz)
time (s)
FliI
FliJ
FliC:FliS
ovalbumin
FliC

Fig. 4

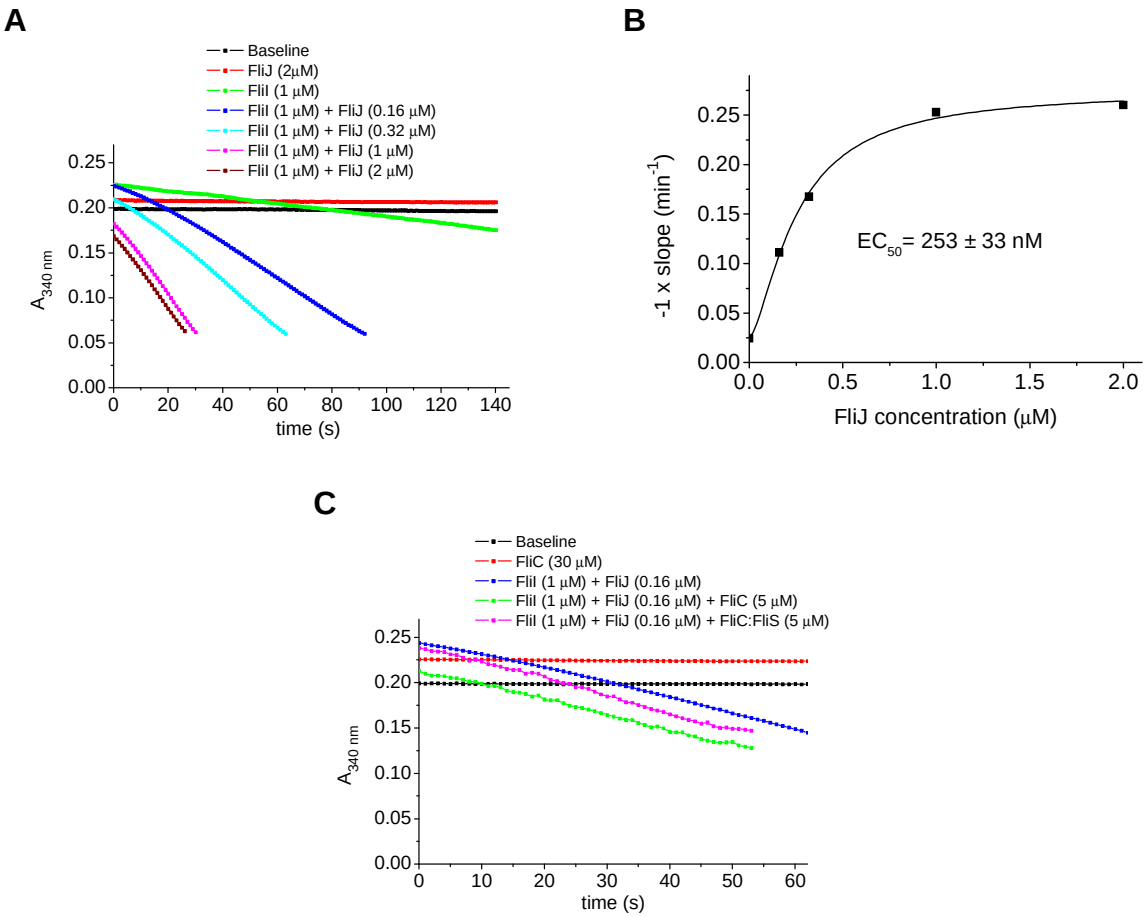
A
Baseline
FliJ (2μM)
FliI (1 μM)
FliI (1 μM) + FliJ (0.16 μM)
FliI (1 μM) + FliJ (0.32 μM)
FliI (1 μM) + FliJ (1 μM)
FliI (1 μM) + FliJ (2 μM)
A340 nm
time (s)
B
-1 x slope (min-1)
EC50= 253 ± 33 nM
FliJ concentration (μM)
C
Baseline
FliC (30 μM)
FliI (1 μM) + FliJ (0.16 μM)
FliI (1 μM) + FliJ (0.16 μM) + FliC (5 μM)
FliI (1 μM) + FliJ (0.16 μM) + FliC:FliS (5 μM)
A340 nm
time (s)

Fig. 5

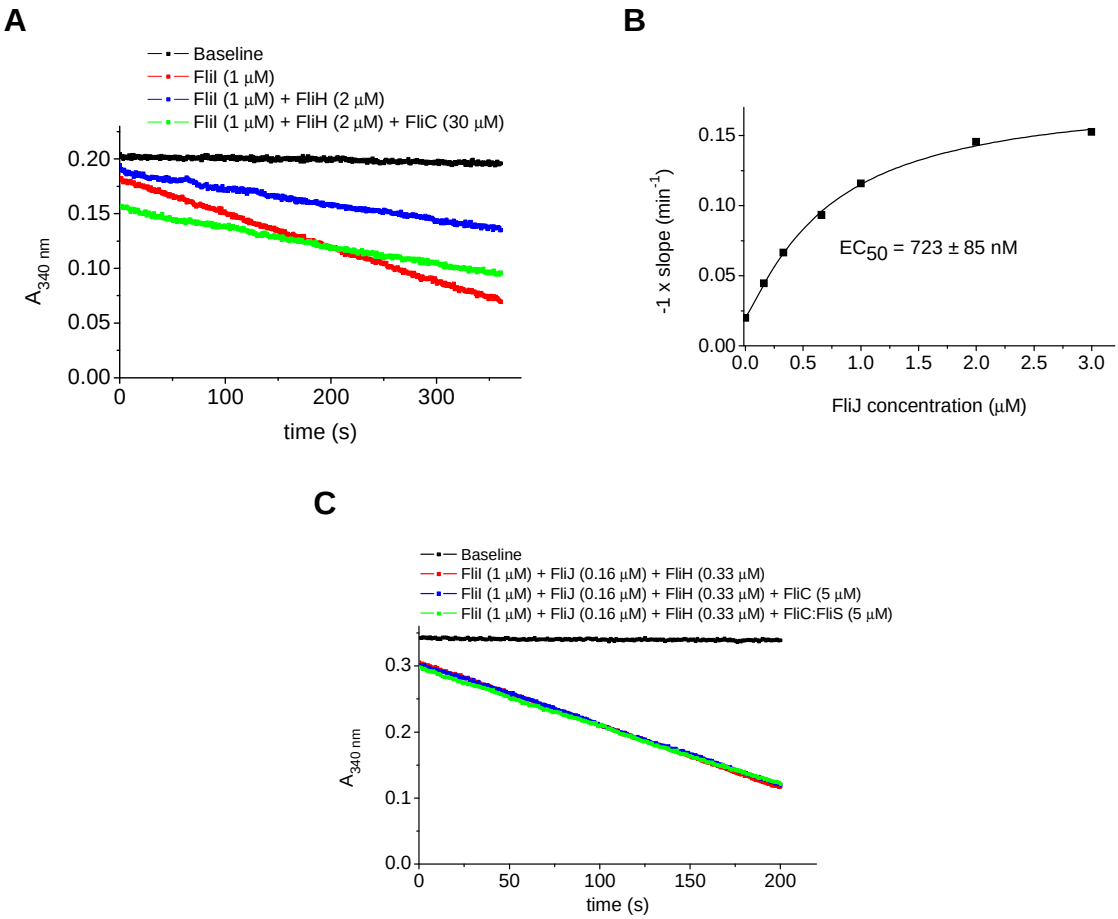
A
Baseline
FliI (1 μM)
FliI (1 μM) + FliH (2 μM)
FliI (1 μM) + FliH (2 μM) + FliC (30 μM)
A340 nm
time (s)
B
-1 x slope (min-1)
EC50 = 723 ± 85 nM
FliJ concentration (μM)
C
Baseline
FliI (1 μM) + FliJ (0.16 μM) + FliH (0.33 μM)
FliI (1 μM) + FliJ (0.16 μM) + FliH (0.33 μM) + FliC (5 μM)
FliI (1 μM) + FliJ (0.16 μM) + FliH (0.33 μM) + FliC:FliS (5 μM)
A340 nm
time (s)

Fig. 6

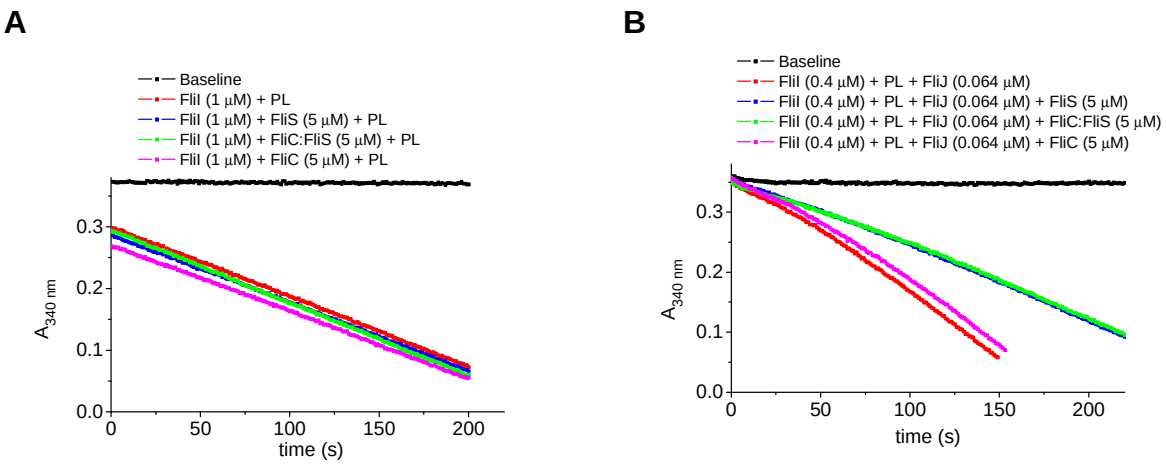
A
Baseline
FliI (1 μM) + PL
FliI (1 μM) + FliS (5 μM) + PL
FliI (1 μM) + FliC:FliS (5 μM) + PL
FliI (1 μM) + FliC (5 μM) + PL
A340 nm
0.0
0.1
0.2
0.3
0
50
100
150
200
time (s)
B
Baseline
FliI (0.4 μM) + PL + FliJ (0.064 μM)
FliI (0.4 μM) + PL + FliJ (0.064 μM) + FliS (5 μM)
FliI (0.4 μM) + PL + FliJ (0.064 μM) + FliC:FliS (5 μM)
FliI (0.4 μM) + PL + FliJ (0.064 μM) + FliC (5 μM)
A340 nm
0.0
0.1
0.2
0.3
0
50
100
150
200
time (s)